

^1H NMR in *a*-Si

W. E. Carlos and P. C. Taylor

Naval Research Laboratory, Washington, D. C. 20375

(Received 19 March 1982)

Results of pulsed NMR studies of hydrogen in *a*-Si:H prepared at several laboratories by glow discharge of silane are presented. The origins of the two ^1H NMR lines seen in almost all samples of *a*-Si:H are discussed. Solid-echo measurements are presented which indicate that these two components are due to spatially isolated groups of protons. We attribute the narrow line to protons slightly clustered in the bulk of the material and the broad line to protons distributed on internal surfaces. The spin-lattice relaxation time shows a minimum at $T \approx 30$ K which is interpreted as due to relaxation via spin diffusion to a small number of H_2 molecules acting as relaxation centers. Annealing results suggest that all the hydrogen molecules are trapped in very similar sites.

I. INTRODUCTION

Amorphous silicon prepared without the inclusion of hydrogen has a large number of dangling bonds (10^{19} to 10^{20} cm^{-3}) and hence a large number of electronic states in the gap which makes it a poor photoconductor of little technological significance.¹ The incorporation of 5–15 at. % hydrogen into the silicon matrix serves to pacify these dangling bonds, thereby removing the states from the gap. While this simple picture of the role of hydrogen is widely accepted, there is still considerable controversy over the hydrogen bonding within the amorphous silicon, the dynamics of the hydrogen-hydrogen interactions, and the interactions of the hydrogen with the amorphous matrix. In this paper we report results of pulsed proton magnetic resonance experiments. Results and conclusions are compared with those obtained by other techniques as well as with those inferred from previous NMR studies.

Hydrogenated amorphous silicon (*a*-Si:H) films are commonly produced by glow discharge of silane (SiH_4) or by rf sputtering of Si in an atmosphere of argon and hydrogen. These processes yield films which are quite similar electronically and structurally. In this paper, we discuss measurements on glow-discharge films. Hydrogenated amorphous Si has been studied extensively using a wide variety of experimental techniques. Transmission electron microscopy² and small-angle x-ray³ and neutron⁴ scattering indicate that many of the films contain voids with typical sizes ranging between 10 and 1000 Å. These results lead to the natural conclusion that at least some of the hydrogen is bonded on the internal surfaces of these voids.

The actual bonding configurations for the hydrogen have been indirectly probed by hydrogen evolution studies.⁵ As the amorphous silicon is heated the rate of hydrogen evolution peaks at ~ 350 , ~ 600 , and ~ 650 °C, where the film starts to crystallize. This behavior is reminiscent of a similar two-phase behavior seen for hydrogen adsorbed on the Si(100) surface.⁶ The fully saturated surface shows dihydride bonding (two hydrogen atoms per surface Si atom) with a (1×1) low-energy electron diffraction (LEED) pattern. Heating the surface to ~ 350 °C causes half the hydrogen to desorb leaving a monohydride surface which reconstructs to give the (2×1) LEED pattern also seen for clean Si(100) surfaces. Heating the surface to ~ 600 °C causes the remaining hydrogen to desorb. Careful preparation, primarily the use of hot substrates, allows one to produce *a*-Si:H films which show little or no low-temperature evolution (≤ 500 °C). Similarly, if the Si(100) is exposed to hydrogen at ~ 300 °C, the dihydride phase is not observed.

Films of *a*-Si:H have been extensively studied with the use of infrared spectroscopy.⁷ These studies have shown the existence of SiH_2 and SiH_3 vibrational modes as well as SiH modes. However, it is seen that high-quality films have very little of the SiH_2 or SiH_3 bands.

NMR studies by Reimer *et al.*^{8,9} and the present authors^{10,11} indicate the existence of two distinct hydrogen environments, isolated from each other. These two environments are manifested in the NMR experiments as a narrow [full width at half maximum (FWHM) ~ 4 kHz] Lorentzian line superimposed on a broad (FWHM ~ 25 kHz) Gaussian line. While small sample-to-sample variations are

seen in the linewidths, these two NMR lines are present in *all* reported results. The samples studied have been prepared with a wide variety of different deposition parameters as well as by several different laboratories and still only the two NMR lines representing two different environments are observed. The narrow line can be explained by a distribution of relatively isolated monohydride sites within the silicon lattice, while the broad line is attributed to various defect sites such as internal surfaces, and in some films, polyhydride species. Clearly a more precise picture of the role of different bonding configurations in these two NMR lines is important to a fundamental understanding of the role of the hydrogen in these films.

The spin-lattice relaxation time T_1 of the protons has been studied over a wide temperature range (4 K to as high as 800 K). All glow-discharge films studied have shown a minimum in T_1 at about 30 K which is relatively independent of frequency, although T_1 is frequency dependent at low temperatures.¹⁰ These results were originally explained by a model in which a small number of hydrogen atoms associated with disorder modes act as relaxation centers, while the rest of the hydrogen is relaxed by spin diffusion to these centers.¹⁰ More detailed calculations of Movaghar and Schweitzer¹² have shown that this interpretation requires $\sim 10\%$ of the hydrogen atoms to be in disorder modes. This number of atoms should be observable directly but no direct observation has been made. Conradi and Norberg¹³ have recently proposed a model in which trapped molecular hydrogen molecules act as the relaxation centers. Recent work¹⁴ of the present authors, which will be detailed in a later section, supports this model. Additional experiments on similar films by Reimer *et al.*⁹ support the basic picture of a small number of relaxation centers with the bulk of hydrogen being relaxed via a spin-diffusion process. It should be pointed out that the T_1 minimum is not seen in some sputtered films.^{14,15}

II. EXPERIMENTAL METHODS

A. Sample preparation

Samples of *a*-Si:H films were obtained from the University of Chicago, RCA Research Laboratories, Brookhaven National Laboratory, and the Naval Research Laboratory and are denoted CHI, RCA, BNL94 and BNL95, and NRL, respectively. All were prepared by rf discharge of silane and deposited onto a hot substrate ($\sim 250^\circ\text{C}$) and contain 10–15 at. % hydrogen. Details of the particular preparation parameters are given in Table I. All samples contained < 0.5 at. % oxygen and < 0.1 at. % nitrogen except for BNL95, which was intentionally doped with ~ 2 at. % oxygen and ~ 0.1 at. % nitrogen. All samples exhibited a small electron spin resonance (ESR) signal ($\lesssim 10^{16}$ spins cm^{-3}).

Samples for NMR were prepared by flaking the films off the substrates or by dissolving the Pyrex or aluminum substrates in HF or HCl, respectively. The amorphous silicon film was packed into a standard quartz ESR tube which was then evacuated and sealed. Typical samples contained from 10 to 100 mg of material. Although we were initially concerned about the effects of the acid treatment, no residual impurities such as fluorine were detected. Furthermore, one sample was simply scraped off the glass substrate and no significant difference could be seen between this sample and those prepared by dissolving the substrate.

B. NMR measurements

The NMR measurements were made using a pulsed NMR spectrometer with a 12-in. Varian magnet. rf pulses were generated by a Matec 5100 main frame with either a Matec 515 or 525 gated amplifier plugin and a Wavetek 3001 cw source.

TABLE I. Growth parameters of *a*-Si:H films.

Sample	Thickness (μm)	Substrate temp. ($^\circ\text{C}$)	Growth rate ($\text{Å}/\text{min}$)	Pressure (Torr)	Power W/cm^2	System type	Gas mixture (mol % silane)	Approximate substrate area (cm^2)	Electron spin density (cm^{-3})
NRL	0.4–10	250	~ 350	0.1–1.0	≤ 1	inductive ^a	1.5	46	7×10^{15}
RCA	~ 1	330	~ 300	0.5	0.1	dc proximity	100	81	5×10^{15}
CHI	~ 10	~ 230	~ 150	0.2	~ 0.4	capacitive	100	~ 25	4×10^{16}
BNL94	~ 6	270	~ 100	0.25	0.1	capacitive	100	500	8×10^{15}
BNL95	~ 6	270	100	0.15	0.1	capacitive	100	500	2×10^{16}

^aCoupling is nominally inductive but because of large diameter there are substantial capacitive effects.

The pulses were fed into the sample coil through a two-capacitor matching network. Phase-sensitive detection was accomplished by a Matec 625 broadband receiver and a tuned preamplifier. Signal averaging was done using either a Nicolet 1074 signal averager with a Biomation Model 805 digitizer or a Nicolet 1170 signal averager.

Typical $\pi/2$ pulse widths were about 1.5 μ sec. Line shapes were determined by Fourier transforming the free induction decay. Spin-lattice relaxation times were found using the repetition-rate method.¹⁶ In all cases the intensity as a function of repetition rate could be fit by a single exponential.

III. GENERAL THEORY

For a detailed discussion of the theory of NMR the reader is referred to any of several texts on the subject.¹⁷ Here we merely outline those aspects which are most relevant to the present work.

The Hamiltonian for spin- $\frac{1}{2}$ nuclei, such as the protons in *a*-Si:H, may be written as the sum of the Zeeman, dipole-dipole, and chemical shift interactions,

$$H = H_Z + H_D + H_C \quad (1)$$

For this system $H_Z \gg H_D \gg H_C$. Furthermore the Zeeman and chemical shift terms only determine the value of the central resonance frequency. The line-shape and relaxation mechanism are due to the dipole-dipole term. For a system of spin- $\frac{1}{2}$ nuclei the second moment due to the dipole-dipole interaction is given by

$$M_2 = (9/20)\gamma^4 \hbar^2 \sum (1/r_{ij}^6), \quad (2)$$

where γ is the nuclear gyromagnetic ratio and r_{ij} is the internuclear distance. If we assume a Gaussian line shape, the linewidth (full width at half maximum) is given by

$$\sigma(\text{FWHM}) = (8 \ln 2 M_2)^{1/2}. \quad (3)$$

For later comparison, Table II gives the linewidths calculated for a number of possible proton distributions.

For more dilute systems the line shape is more Lorentzian.¹⁸ The method of moments cannot be used for a Lorentzian line since the second and all higher moments diverge. For such systems there are a number of calculations of the line shape.^{19,20} It is not our intention to evaluate the merits of the various calculations as they do not differ any more than ~20% in predicted linewidth. The statistical theory¹⁹ gives the linewidth (FWHM) as

TABLE II. Calculated ¹H NMR linewidths for different proton distributions.

Bonding arrangement	σ (kHz) ^a
SiH ₂	13.4 ^b
SiH ₃	19 ^c
Si(111):H	8.5 ^c
C-Si hydrogenated monovacancy	114 ^c
C-Si hydrogenated divacancy	94 ^c
Uniform array	0.28/at. % ^d
Random array	0.46/at. % ^d

^aFull width at half maximum.

^bThis is the width of a Pake doublet due to SiH₂.

^cAssumes a Gaussian shape.

^dAssumes a cubic lattice.

$$\sigma(\text{FWHM}) = (4\pi^2/3\sqrt{3})\gamma^2 \hbar n, \quad (4)$$

where n is density of spins. For amorphous silicon this yields about 460 Hz per atomic percent hydrogen.

Spin-lattice relaxation requires an energy sink as well as a coupling to the magnetic moment of the

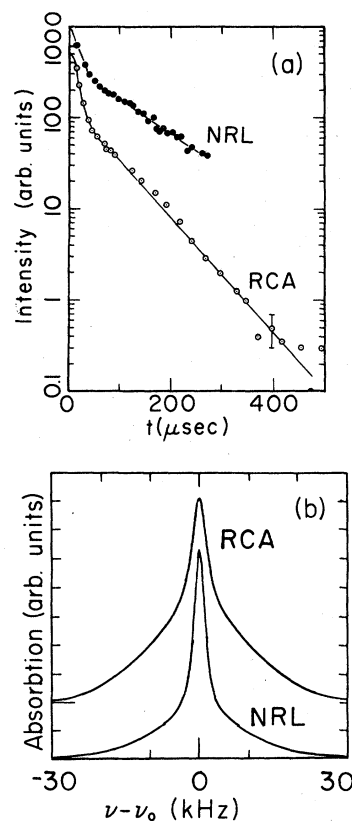


FIG. 1. (a) Free induction decays (FID's) for two representative samples. (b) Line shapes for two samples obtained by Fourier transforming the FID's in (a).

proton. A number of different mechanisms are known to produce a minimum in the spin-lattice relaxation time T_1 with temperature as is observed¹⁰ in *a*-Si:H. These mechanisms include paramagnetic centers, physical motion of the protons, and disorder modes as conceivable relaxation mechanisms for this system. The possibilities will be discussed in light of the T_1 data.

IV. RESULTS

A. The NMR line shape

The line shape is determined by Fourier transforming the free induction decay (FID) which occurs after a 90° pulse is applied. Two representative FID's and the corresponding line shapes are shown in Figs. 1(a) and 1(b), respectively. Although some subtle differences can be seen in the two FID's it is apparent that they are quite similar. The FID is composed of two components: an exponential decay at long times which transforms to a narrow Lorentzian line in the frequency domain and at short times, a Gaussian shape which transforms to a broad Gaussian line. The linewidths and relative intensities of the two lines for the various samples are listed in Table III. Hole burning experiments by Reimer *et al.*,⁸ as well as our own solid-echo experiments to be described below, clearly indicate that there are two separate sites giving rise to the two lines. As can be seen in Table III, there is very little variation in the two linewidths from sample to sample. Although they were prepared at four different laboratories, it is not too surprising that there should be so little variation because the deposition conditions and hydrogen content are similar. What is quite remarkable though is that previous work of Reimer *et al.*,^{8,9} Lowry *et al.*,¹⁵ Ueda *et al.*,²¹ and the present authors on both glow-discharge and sputtered films prepared under a wide variety of

TABLE III. NMR line shape parameters for *a*-Si:H samples.

Sample	σ_L (kHz) ^a	σ_G (kHz) ^a	Intensity ratio (broad/narrow)
RCA	3.8	26	3.2
NRL	2.7	22	1.3
CHI	3.4	32	3.1
BNL94	2.4	23	1.7
BNL95	2.9	26	3.2

^aFull width at half maximum.

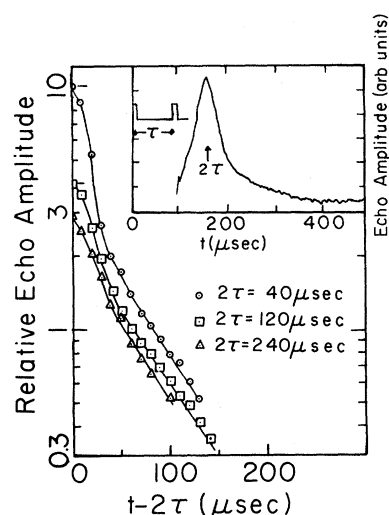


FIG. 2. Solid-echo amplitudes obtained from a 90° - τ - 90° pulse sequence as shown in the inset. Results are compared for three values of 2τ .

deposition conditions, all see only the same two lines of ~ 4 and ~ 25 kHz linewidths.

B. Solid-echo experiments

In order to confirm that the two ^1H lines, which are always observed in *a*-Si:H, do not constitute a homogeneous ensemble of spins, dipolar "solid-echo" experiments²²⁻²⁶ were performed. For an ensemble of spin $I = \frac{1}{2}$ nuclei, it can be shown^{22,25} that an echo results at time $t = 2\tau$ after the application of two 90° pulses (at $t = 0$ and $t = \tau$), where the rf phase of the second pulse is 90° with respect to that of the first. A representative echo at 77 K

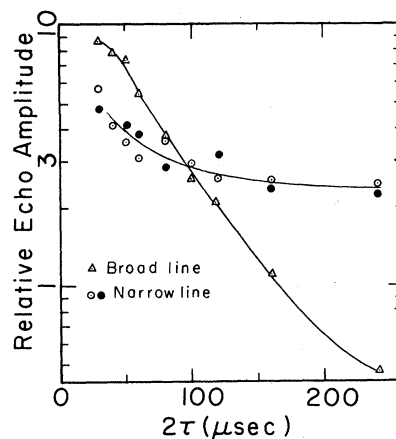


FIG. 3. Decay in the echo amplitude as a function of pulse separation for the broad- and narrow-line components of the echo.

from such a 90° - τ - 90°_{90} pulse sequence applied to a sample of α -Si:H (RCA) is shown in the inset to Fig. 2. The pulse widths, which are exaggerated for clarity in the inset to Fig. 2, were $\leq 2 \mu\text{sec}$. Semi-log plots of echo decays at several representative pulse separations are shown in the main portion of Fig. 2 as functions of $t-2\tau$. The decompositions of these lines into broad Gaussian and Lorentzian components are indicated by the dashed lines.

If significant spin diffusion were occurring during the times probed by these echo measurements ($t=2\tau \leq 300 \mu\text{sec}$), then the echo decay would reflect this fact. In particular, one would expect an equilibrium ratio to be established between the two components at times longer than the effective spin-diffusion time. However, as is apparent from the results of Fig. 3, the two components decay at markedly different rates over all pulse separations measured. In this figure we have plotted (open data points) the intensities of the broad and narrow lines at $t=2\tau$ using extrapolations similar to those illustrated by the dashed lines in Fig. 2. The solid data are a second estimate to the narrow-line decay obtained by plotting the relative signal amplitudes at $t-2\tau=100 \mu\text{sec}$ where the contribution from the broad line is negligible. For comparison, these data have been normalized to the $t=2\tau$ extrapolations at $2\tau=40 \mu\text{sec}$.

One may safely conclude from Fig. 3 that there is negligible spin diffusion between the two lines out to at least $250 \mu\text{sec}$. This conclusion is consistent with those inferred from previous "hole burning" experiments¹⁰ which probed spin-spin effects in α -Si:H on a 1-msec time scale.

Theoretical descriptions of the solid-echo decay with increasing pulse separation are not generally available, but at short times it can be shown that the solid-echo decay can be related to the fourth moment of the line shape.²³ This procedure, which is inappropriate for a line which is purely Lorentzian, should, in principle, be capable of distinguishing small departures from a Gaussian line shape in the wings. Unfortunately, the echo response cannot be observed for $2\tau \leq 25 \mu\text{sec}$ because of the dead time of the NMR spectrometer and the moment expansion breaks down for the region which is experimentally accessible ($2\tau \geq 30 \mu\text{sec}$).

Solid-echo experiments designed to observe isolated, coupled-spin systems^{27,28} were also attempted. For example, isolated pairs of spins with $I = \frac{1}{2}$ can often be treated as a pseudospin ($I=1$) system. Similarly, three protons which exist as an isolated species may behave as a single quasiparticle of spin $I = \frac{3}{2}$ as far as the magnetic resonance is concerned.

These coupled-spin systems, which might be isolated dihydride or trihydride species, could produce "quasi-quadrupolar" echos^{27,28} which depend in predictable ways on the length b and rf phase ϕ of the second pulse in the echo sequence. A systematic investigation which varied both b and ϕ detected no additional echoes in the sample of α -Si:H. This result does not imply that there are no SiH_2 or SiH_3 groups in the sample, but merely that there are few isolated dihydride and trihydride groups.

C. Spin-lattice relaxation

The spin-lattice relaxation time T_1 provides a measure of the rate at which the spin system returns to equilibrium by releasing energy to the surrounding lattice. We have measured T_1 as a function of frequency and temperature. In this section we cover results for $T < 300 \text{ K}$ and defer a discussion of our results at elevated temperatures to the next section. Before giving details about particular results a few general points should be made. In all samples studied no aging effects were seen either as changes

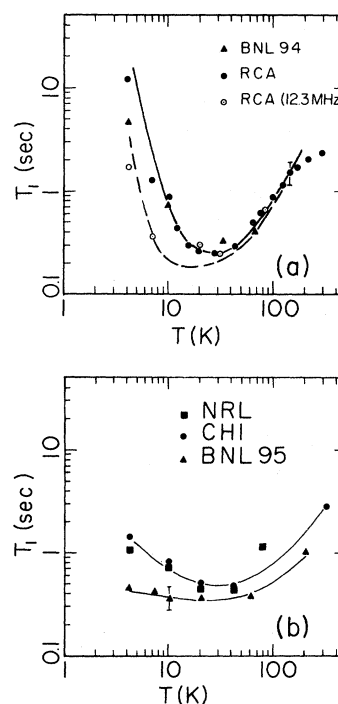


FIG. 4. (a) T_1 as a function of temperature for RCA and BNL94 at $\nu_0=42.3 \text{ MHz}$ and for RCA at 12.3 MHz . The curves are obtained from a fit to the model of Conradi and Norberg (Ref. 13). (b) T_1 as a function of temperature for NRL, CHI, and BNL95 ($\nu_0=42.3 \text{ MHz}$). Curves are drawn as an aid to the eye.

in T_1 or the line shape. The T_1 's were measured by the repetition-rate method and in all cases the decay was exponential over 1 to 2 orders of magnitude. Furthermore, both lines have the same T_1 within the accuracy of our measurements (about $\pm 10\%$).

Figures 4(a) and 4(b) show T_1 as a function of temperature at 42.3 MHz for several samples. The temperatures are accurate to ± 1 K, which is a significant uncertainty only at the lowest temperatures. As might be expected, since all the films were deposited under similar conditions, the dependence of T_1 on temperature is quite similar. All have a minimum in T_1 as a function of temperature at $T \approx 30$ K, and in all cases the magnitude of T_1 varies from a few seconds to a few tenths of a second. While there are considerable similarities between the various samples some differences are also apparent. The samples prepared at the University of Chicago and at NRL both have shallower minimums and a less rapid increase in T_1 with decreasing temperature below the minimum than does the sample from RCA or the relatively oxygen-free samples from Brookhaven. In many respects the T_1 results for the NRL and Chicago samples are quite similar to those for BNL95, which was intentionally doped with ~ 1.5 at. % oxygen.

Figure 5 gives the frequency dependence of the RCA sample at a low temperature (~ 5 K) and at a relatively high temperature (77 K). At low temperature, T_1 shows an approximately linear dependence on frequency. For temperatures above the minimum no frequency dependence is seen. Furthermore, as can be seen in Fig. 4(a), the frequency dependence has disappeared above the temperature of the minimum. While we have not investigated the frequency dependence of T_1 for all samples as thoroughly as this one, a check of T_1 for $\nu_0 \approx 15$ MHz indicates that all follow the same trend.

D. High temperature and annealing

The effects of annealing on both the line shape and the temperature dependence of the spin-lattice

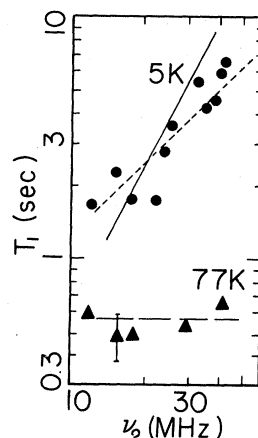


FIG. 5. T_1 as a function of frequency at ~ 5 and 77 K. The solid and short dashed lines are fits of the 5-K data to quadratic and linear dependences on ν_0 , respectively.

relaxation time were investigated for one sample of α -Si:H (RCA). In addition, T_1 was measured at elevated temperature during the annealing process.²⁹ The sample was held at each elevated temperature for about six hours while the measurements were performed. Subsequent measurements at temperatures below 300 K were performed after annealing at most temperatures.

Measurable hydrogen was driven off at temperatures above $\sim 400^\circ\text{C}$. Table IV summarizes the effects of annealing on the NMR line shape and the hydrogen content. The annealing narrows both the broad and narrow lines due to an increase in average hydrogen-hydrogen separation. The concentration of hydrogen in the more clustered region (broad line) decreases more rapidly than in the less clustered region (narrow line). Earlier annealing results by Reimer *et al.*³⁰ on a film prepared at room temperature containing ~ 21 at. % hydrogen differ from our results in several aspects: (1) We see no redistribution of hydrogen from the broad line into the narrow line. (2) We do not see changes in linewidths as large as these authors did, e.g., the linewidth of the narrow component has dropped to ~ 500 Hz by 500°C in the work of Reimer *et al.*,

TABLE IV. Effects of annealing α -Si:H (RCA).

Annealing temp. ($^\circ\text{C}$)	Linewidth ^a (narrow line)	Linewidth ^a (broad line)	Intensity ratio (broad/narrow)	Total H (at. %)	Electronic spins (cm^{-3})
(Before annealing)	3.7 kHz	25.6 kHz	3.2	12	5×10^{15}
450	2.5 kHz	21.0 kHz	2.5	7	4×10^{17}
500	2.0 kHz	15.0 kHz	2	4.7	2×10^{18}
530	1.8 kHz		0	1.3	7×10^{18}

^aFull width at half maximum.

while in our case the linewidth is ~ 2 kHz after a similar anneal. (3) There is no evolution of hydrogen below $T \approx 400^\circ\text{C}$ in our work, while Reimer *et al.* report a drop from ~ 20 to ~ 12 at. % between $T = 300$ and 400°C . This latter disagreement is perhaps least surprising since our film was grown on a substrate held at $T = 330^\circ\text{C}$ rather than room temperature. Interestingly, the hydrogen concentration as a function annealing temperature is about the same for the two films for $T > 400^\circ\text{C}$. The first two discrepancies are no doubt also due to differences in growth conditions for the samples.

The spin-lattice relaxation rate ($1/T_1$) at elevated temperatures is given in Fig. 6. Above $T \approx 300^\circ\text{C}$ the rate increases with increasing temperature. We suggest that this increase in rate is due to some local motion of the hydrogen precursory to actual motion of hydrogen out of the sample. One would not expect to see a motional narrowing of the line below approximately the temperature at which the rate reaches a maximum, which is not experimentally attainable. Although there is some scatter in the data, the general increase gives an activation energy of ~ 0.2 eV. We obtain the same activation energy from the changes in the narrow line with annealing temperature.²⁹ This energy agrees reasonably well with previous work of Reimer *et al.* who found an activation energy of 0.3 eV from the changes in the narrow line width with annealing temperature. Activation energies from ~ 0.2 to ~ 1.7 eV may be deduced from published hydrogen evolution data^{4,31} and so it is difficult to make any quantitative comparison with those results.

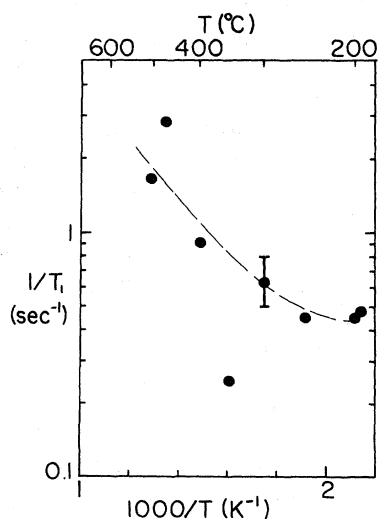


FIG. 6. Spin-lattice relaxation rate ($1/T_1$) at high temperatures. The line is drawn to aid the eye.

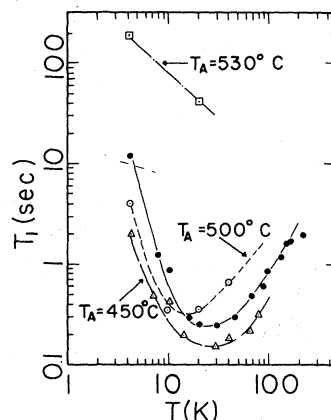


FIG. 7. Low-temperature T_1 minimum after annealing. The curves are drawn merely as a visual aid. The data prior to annealing (solid points) are included for reference.

After several of the higher-temperature anneals we again looked at the T_1 minimum. The results, shown in Fig. 7, show little change in the low-temperature minimum up to $T_A = 500^\circ\text{C}$ even though about two thirds of the hydrogen has evolved by that time. However, after annealing the sample at 530°C the minimum has disappeared, which indicates that the relaxation centers must all be in quite similar environments to evolve over such a narrow temperature range.

V. DISCUSSION

It is clear that an understanding of the origins of the two NMR lines and their ubiquitous appearance is of fundamental importance to an understanding of the hydrogen bonding in amorphous silicon. It is generally accepted that the narrow Lorentzian line is due to hydrogen atoms placed randomly in the amorphous silicon network at "monohydride" sites. Table II gives a (Lorentzian) linewidth of about 3.5 kHz for a concentration of 8 at. % based on a statistical calculation for a system of spins randomly placed on a cubic lattice. Since the narrow line is due to at most $\frac{1}{2}$ of the hydrogen (i.e., < 6 at. %), the protons which contribute to the narrow line must be clustered in regions of relatively higher concentration with other regions having little or no hydrogen. For some samples such as NRL and BNL94, which have a relatively large amount of hydrogen (4–6 at. %) in the narrow line, this line is reasonably accounted for by a random distribution of sites over $\sim 75\%$ of the lattice. However, the other three samples (RCA, CHI, and BNL95) have

less hydrogen (~ 3 at. %) in the narrow line and yet somewhat larger linewidths. At least in these samples the hydrogen must be clustered in the region not occupied by the protons giving rise to broad line. Reimer *et al.*⁹ estimated that about 25% of the lattice was occupied either by protons giving rise to the broad line or by "buffer" regions between the broad-line and narrow-line regions. Reimer *et al.*⁹ had calculated that the narrow line could be accounted for by a random distribution of spins with no clustering. However, their calculation is based on fitting the line to a Gaussian form, whereas the present calculation is based on a Lorentzian line shape, which is much closer to that which is observed.

The interpretation of the broad line is not so clear cut. In the present study none of the films show any appreciable infrared absorption which is not attributable to monohydride vibrations.³² Furthermore the broad line is too narrow to be due primarily to hydrogenated vacancies or divacancies. Although one would expect the silicon atoms to relax around a vacancy, the magnitude of this relaxation must be ≥ 0.5 Å to give a linewidth of about 25 kHz, and this magnitude is probably unreasonable. The most likely interpretation is that the broad line is due to hydrogen bonded on the internal surfaces of small voids with typical dimensions of 5 to 100 Å. It is natural to compare the observed linewidth of ~ 25 kHz to that calculated in Table II for crystalline silicon surfaces (~ 8 kHz). By comparing the calculated linewidths for hydrogen in the bulk uniformly and randomly distributed, we see that randomness can significantly increase the linewidth over that which might be expected from an average proton-proton separation. For both (111) and (110) crystalline surfaces, which would have one hydrogen per Si atom, the hydrogen is bonded only to next-nearest-neighbor silicon atoms. One can expect in amorphous silicon to see hydrogen atoms bonded to nearest-neighbor (although those protons would also be ~ 3.8 Å apart) and third-nearest-neighbor silicon atoms in addition to distorted bond angles and bond lengths. Both of these factors will yield a distribution in hydrogen-hydrogen separations instead of the discrete values for the hydrogenated crystalline surfaces. Since the dipolar interaction decreases as r^{-6} we need only consider nearest-neighbor spins in calculating a reasonable estimate of the second moment using Eq. (2), i.e.,

$$M_2 \propto 1/d^6, \quad (5)$$

where d is the crystalline surface proton-proton separation [3.84 Å on Si(111)]. For simplicity we

will take x to have a rectangular distribution from $d + \Delta d$ to $d - \Delta d$. The random nature of the distribution will then increase the second moment by a factor β given by

$$\beta = (M_2^A / M_2^C) = \frac{1}{10Y} \left[\frac{1}{(1-Y)^5} - \frac{1}{(1+Y)^5} \right], \quad (6)$$

where M_2^A , M_2^C are the second moments for amorphous and crystalline surfaces, respectively, and $Y = \Delta d / d$. A value of $Y \approx 0.5$ is required to increase the crystalline linewidth to that which is observed. This calculation assumes that the mean separation (i.e., the density) is the same as in the case of the crystalline surface and naturally the width of the distribution could be somewhat reduced by assuming that the amorphous surface is more densely packed. There seems to be little reason to believe that the internal amorphous surfaces are denser than the crystalline surfaces, especially since the principal crystalline surfaces all have similar densities. While this may seem to be a very broad distribution in nearest-neighbor proton-proton separation it does help to explain one rather puzzling observation. For those films which show SiH_2 , SiH_3 , and $(\text{SiH}_2)_n$ vibrations, no new proton NMR line is observed⁹ even though the nearest-neighbor proton-proton distance is 2.45 Å for these bonding configurations. If we do assume that a broad distribution of nearest-neighbor "monohydride" distances exists along with the polyhydride groups it is not surprising that the addition of such groups to the film does not change the linewidth appreciably. In addition, since we assume the voids to be irregularly shaped it is only natural to expect that there are "corners" or "edges" to the void where the protons would be quite close together. To summarize this point, a rather broad distribution of proton-proton separations on the internal surfaces is necessary to account for the width of the broad line. However, by assuming such a distribution we obtain a natural explanation of why such groups as SiH_2 do not give rise to an additional line.

In considering various possible models for the spin-lattice relaxation mechanism it is worthwhile to reemphasize the features of the data which must be fit. The most prominent features are the minimum in T_1 at $T \approx 30$ K and the relatively strong frequency dependence of T_1 at low temperatures. Any proposed mechanism must also be able to fit the magnitude of T_1 with a reasonably small number of relaxation centers. A number of mechanisms have been shown to give T_1 minima in

other solids. Actual motion of the protons would produce a T_1 minimum.³³ However, this would also yield a narrowing of the NMR line at temperatures above the minimum, while the observed NMR line is independent of temperature. Paramagnetic impurities could, in principle, produce a minimum.³⁴ However, to yield a minimum at $T \approx 30$ K one would need a large density ($\sim 10^{19}$ cm⁻³) of a very rapidly relaxing center such as a non-*s*-state ion. Secondary-ion mass-spectroscopy analysis³² (SIMS) and our own electron spin resonance (ESR) data clearly indicate that there are not nearly enough of such impurities to give such a rapid relaxation. Raman processes involving phonons and/or disorder modes have been invoked to account for T_1 minima³⁵ seen in other amorphous solids. Such a mechanism would yield a T_1 which was independent of frequency, contrary to our results. Relaxation via dangling bonds¹¹ or other localized electronic centers¹⁵ has been proposed for hydrogen in some sputtered *a*-Si:H films. However, these give no minimum in T_1 . The present authors originally proposed that a small fraction of the hydrogen atoms in disorder modes would act as relaxation centers.¹⁰ Recently Movaghar and Schweitzer,¹² using a more refined calculation, have pointed out that approximately 10% of the hydrogen atoms would have to be in a disorder mode to yield the observed relaxations times. Such a large number of centers should be directly observable, and there is no direct evidence.

Conradi and Norberg (hereafter referred to as CN) have recently proposed that molecular hydrogen trapped in the silicon matrix acts as the relaxation center.¹³ We have recently published results which support this model.¹⁴

In the model proposed by CN a small number of hydrogen molecules ($\sim 1\%$ of the total hydrogen in the lattice) acts as relaxation centers with the bonded hydrogen relaxing via spin diffusion. The relaxation of the molecular hydrogen produces the minimum in T_1 . The mechanism is the same as has been used to explain the relaxation of molecular hydrogen in rare-gas solids.³⁶ For the bonded hydrogen the spin-lattice relaxation time is given as

$$T_1(\text{H}) = \frac{3}{8} T_1(\text{H}_2) [n(\text{H})/n(o\text{-H}_2)] + T_1(\text{SD}), \quad (7)$$

where $n(\text{H})$ is the total concentration of hydrogen in the sample and $n(o\text{-H}_2)$ is the concentration of orthohydrogen in the material. $T_1(\text{H}_2)$ is the spin-lattice relaxation time for the orthohydrogen molecules, and $T_1(\text{SD})$ is a spin-diffusion limited term which can produce a spin-diffusion bottleneck. The

factor $\frac{3}{8}$ is due to different nuclear spins of the hydrogen atom ($I = \frac{1}{2}$) and the orthohydrogen molecule ($I = 1$). The relaxation rate for the orthohydrogen is given as

$$\frac{1}{T_1(\text{H}_2)} = \frac{3}{5} n_r \omega_d^2 \left(\frac{\tau}{1 + \omega_0^2 \tau^2} + \frac{4\tau}{1 + 4\omega_0^2 \tau^2} \right), \quad (8)$$

where $\omega_d = 3.6 \times 10^5$ sec⁻¹ is the dipolar coupling between the protons in an H₂ molecule, τ^{-1} is the rate at which the lattice induces rotational transitions in the H₂ molecule, and ω_0 is the resonant frequency. There are a total of eight rotational modes which couple to the nuclear spin system.³⁷ Electric field gradients at the site will shift the energy of all but n_r of these modes away from $\hbar\omega_0$. For a site of low symmetry (the case assumed by CN) $n_r = 2$, for axial symmetry $n_r = 4$, and for a high-symmetry site with no field gradients $n_r = 8$. Conradi and Norberg assume that the rate τ^{-1} is that for a quadrupolar nucleus relaxing via a two-phonon Raman process.¹³ Clearly the functional dependence of τ is not relevant to the value of T_1 at the minimum or to the frequency dependence of T_1 at either low temperatures (high τ) or high temperatures (low τ). $T_1(\text{H}_2)$ is calculated to be ~ 1 nsec at the minimum^{13,38} and $T_1(\text{SD})$ is taken to be ~ 0.16 sec. Therefore, $\sim 1\%$ of the hydrogen must be in molecular form to give the observed minimum in T_1 .

One test of this model is to look for the conversion of the orthohydrogen to parahydrogen, which does not act as a relaxation center because $I = 0$. This conversion is a slow bimolecular process driven by the interaction between protons on adjacent H₂ molecules.³⁷ The ortho-to-para ratio will be frozen in during the normal running of an experiment. In order to test for this effect we held a sample (RCA) at liquid-helium temperature for three months and intermittently checked for changes in the T_1 minimum. The results are displayed in Fig. 8 which shows an increase in the minimum as a function of the time held at 4.2 K.

As mentioned before, this conversion is bimolecular and hence described by the equation

$$\frac{dx_0}{dt} = -Cx_0^2, \quad (9)$$

where x_0 is the fraction of H₂ molecules in the ortho state and C is the rate constant. The value of T_1 at a given temperature will be linear in time since it is inversely proportional to x_0 . This is shown in Fig. 9 for $T = T_{\text{min}}$. Annealing the sample at room temperature restored the values of T_1

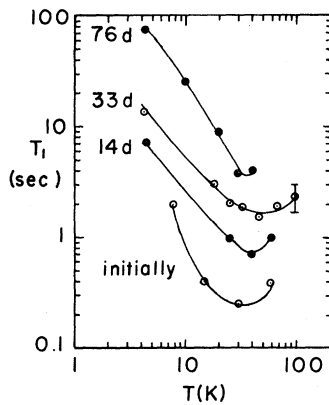


FIG. 8. Effect on the T_1 minimum of holding the sample (RCA) at 4.2 K for the time indicated on the left.

initially measured.

Although the molecular hydrogen model does fit the T_1 vs temperature data quite well there are a number of difficulties which deserve mention. The CN model gives an ω^2 frequency dependence, but the data are better fit by a linear frequency dependence although there is significant scatter. Also, several samples (BNL95, NRL, and CHI) have much weaker temperature dependences for $T < T_{\min}$ than the others. In the CN model, $T_1 \propto T^{-7}$ at low temperatures. This temperature dependence arises from the relaxation of the H_2 molecule to the lattice via a two-phonon Raman process.^{38,39} In addition to phonons, many amorphous materials contain low-energy localized excitations known as disorder modes or two-level systems.⁴⁰ In these solids there exist atoms or groups of atoms which may tunnel or

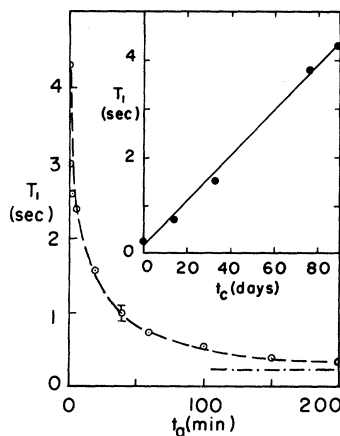


FIG. 9. Change in the value of T_1 (min) as a function of the time held at 4.2 K (inset) and the return of the value of T_1 (min) as a function of time (t_a) annealed at room temperature.

hop between two local-energy minima. The energy distribution of these disorder modes is roughly constant at low energies in most materials.⁴⁰ Reinecke and Ngai⁴¹ have shown that Raman processes involving two disorder modes yield a spin-lattice relaxation time proportional to T^{-1} at low temperatures,⁴¹ while Raman processes involving a phonon and a disorder mode yield a T^{-4} dependence. While our data are insufficient to distinguish between a T^{-7} and a T^{-4} temperature dependence for T_1 of the RCA and oxygen-free Brookhaven samples, the temperature dependence is clearly stronger than T^{-1} . However, the other samples (BNL95, NRL, and CHI) have much weaker temperature dependences and therefore it is possible that in these films Raman processes involving disorder modes provide the dominant mechanism for relaxing the H_2 molecules. Although the oxygen content of samples NRL and CHI is not well documented, the BNL95 film contains more oxygen than do RCA and BNL94. Because ultrasonic measurements⁴² indicate that the number of low-frequency disorder modes increases with oxygen content, one might speculate that the disorder modes involved in the relaxation in BNL95 are associated with the oxygen impurity.

These discrepancies are primarily questions concerning the details of the CN model, i.e., of how the hydrogen molecules relax to the lattice, and not of the central point of the model, which is the existence of a small density of H_2 molecules which act as relaxation centers in the glow-discharge deposited a -Si:H films. While the number of H_2 molecules needed is small, this number should be detectable directly by NMR provided its line shape can be differentiated from those due to the bonded hydrogen. One would expect the molecular hydrogen line to be motionally narrowed and therefore easily resolved. However, as can be seen in Fig. 1(a), the free induction can be followed through 3 orders of magnitude and no third line is resolved. It is possible that the molecular hydrogen line is not fully motionally narrowed. The molecules could be confined to move in some localized region where they could still interact with bonded hydrogen. Conradi and Norberg have assumed that the molecular hydrogen sits at a site of low symmetry, if we consider a high-symmetry site this would reduce the number of H_2 molecules necessary by a factor of ~ 4 to a point where they would only be marginally detectable in our experiment.

The annealing data support the concept that the hydrogen molecules all exist in a particular site since all the relaxation centers anneal out between

500 and 530°C. Furthermore, the existence of a small amount of molecular hydrogen trapped in the *a*-Si film is consistent with current models^{43,44} of the growth process for these films. In these models^{42,43} hydrogen is removed from the film during growth as H₂ molecules are formed at the surface. Within this context one might expect to see some of the H₂ trapped within the film in microvoids small enough to trap such a small molecule in an arrangement that is stable up to 500°C. These microstructures are probably not unique to the glow-discharge prepared *a*-Si:H films. Films prepared by sputtering in argon have some argon trapped up to similar temperatures,⁵ and the argon atom is only about 15% larger than H₂.

VI. SUMMARY

The results of a series of NMR experiments on hydrogen in amorphous silicon have been presented. There are two ¹H NMR lines, one associated with hydrogen slightly clustered but distributed essentially throughout the film and a second associated with hydrogen strongly clustered at defects such as internal surfaces. The spin-lattice relaxation time T_1 goes through a minimum at $T \approx 30$ K and shows a roughly linear frequency dependence at low temperatures. The T_1 minimum is reasonably ex-

plained by a model of Conradi and Norberg in which $\sim 1\%$ of the hydrogen is trapped as molecular hydrogen which serves as the relaxation center. Although there are some questions about details of the model, the conversion of the molecular hydrogen from the ortho state to the para state provides convincing support for the general mechanism. The annealing data indicate that the H₂ molecules are trapped in well-defined sites, while the magnitude of the T_1 minimum suggests that these sites are quite abundant ($\sim 10^{19}/\text{cm}^3$) in the amorphous silicon.

ACKNOWLEDGMENTS

The authors thank Professor R. E. Norberg and Professor M. Conradi for helpful discussions. D. E. Carlson and J. Dresner (RCA), H. Fritzsche and C. C. Tsai (University of Chicago), R. W. Griffith (Brookhaven National Laboratory), and P. Reid (Naval Research Laboratory) are thanked for supplying samples used in this work. This work was supported by the Department of Energy under Contract Nos. DE-AI01-79ET23078 and DE-AI02-80-CS-83116. During part of this work one of us (W.E.C.) was supported by an NRL/NRC postdoctoral research associateship.

¹See, for example, *Tetrahedrally Bonded Amorphous Semiconductors, (Carefree, Arizona)*, A Topical Conference on Tetrahedrally Bonded Amorphous Semiconductors, edited by R. A. Street, D. K. Biegelsen, and J. C. Knights (AIP, New York, 1981).

²J. C. Knights and R. A. Lujan, *Appl. Phys. Lett.* **35**, 344 (1979).

³P. D'Antonio and J. H. Konnert, *Phys. Rev. Lett.* **43**, 1163 (1979).

⁴A. J. Leadbetter, A. A. M. Rashid, N. Colenutt, A. F. Wright, and J. C. Knights, *Solid State Commun.* **38**, 957 (1981).

⁵S. Oguz and M. A. Paesler, *Phys. Rev. B* **22**, 6213 (1980); D. K. Biegelsen, R. A. Street, C. C. Tasi, and J. C. Knights, *ibid.* **20**, 4839 (1979).

⁶T. Sakurai and H. Hagstrum, *Phys. Rev. B* **14**, 1593 (1976).

⁷M. H. Brodsky, M. Cardona, and J. J. Cuomo, *Phys. Rev. B* **16**, 3556 (1977); G. Lucovsky, R. J. Nemanich, and J. C. Knights, *ibid.* **19**, 2064 (1979); E. C. Freeman and W. Paul, *ibid.* **18**, 4288 (1978).

⁸J. A. Reimer, R. W. Vaughan, and J. C. Knights, *Phys. Rev. B* **23**, 2567 (1981).

⁹J. A. Reimer, R. W. Vaughan, and J. C. Knights, *Phys.*

Rev. Lett. **44**, 193 (1980); *Phys. Rev. B* **24**, 3360 (1981).

¹⁰W. E. Carlos and P. C. Taylor, *Phys. Rev. Lett.* **45**, 358 (1980); P. C. Taylor and W. E. Carlos, *J. Phys. Soc. Jpn.* **49**, 1193 (1980).

¹¹W. E. Carlos, P. C. Taylor, S. Oguz, and W. Paul, in *Tetrahedrally Bonded Amorphous Semiconductors (Carefree, Arizona)*, A Topical Conference on Tetrahedrally Bonded Amorphous Semiconductors, Ref. 1, p. 67.

¹²B. Movaghar and L. Schweitzer, in *Tetrahedrally Bonded Amorphous Semiconductors (Carefree, Arizona)*, A Topical Conference on Tetrahedrally Bonded Amorphous Semiconductors, Ref. 1, p. 73.

¹³M. Conradi and R. Norberg, *Phys. Rev. B* **24**, 2285 (1981).

¹⁴W. E. Carlos and P. C. Taylor, *Phys. Rev. B* **25**, 1435 (1982).

¹⁵M. Lowry, F. R. Jeffrey, R. G. Barnes, and D. R. Torgeson, *Solid State Commun.* **38**, 113 (1981).

¹⁶S. Alexander and A. Tzalmona, *Phys. Rev.* **138**, A845 (1965).

¹⁷C. P. Slichter, *Principles of Magnetic Resonance* (Springer, New York, 1980); A. Abragam, *The Princi-*

- ples of Nuclear Magnetism* (Oxford University Press, London, 1961).
- ¹⁸C. Kittel and E. Abrahams, *Phys. Rev.* **90**, 238 (1953).
- ¹⁹C. W. Myles, C. Ebner, and P. A. Fedders, *Phys. Rev B* **14**, 1 (1976).
- ²⁰A. Abragam, *The Principles of Nuclear Magnetism* (Oxford University Press, London, 1961), p. 126.
- ²¹S. Ueda, M. Kumeda, and T. Shimizu, *Jpn. J. Appl. Phys.* **20**, L399 (1981).
- ²²I. G. Powles and P. Mansfield, *Phys. Lett.* **2**, 58 (1962).
- ²³I. G. Powles and I. H. Strange, *Proc. Phys. Soc. London* **82**, 6 (1963).
- ²⁴P. Mansfield, *Phys. Rev.* **137**, A961 (1965).
- ²⁵R. Hausser and G. Siegle, *Phys. Lett.* **19**, 356 (1965).
- ²⁶G. Siegle, *Z. Naturforsch.* **23a**, 556 (1968).
- ²⁷P. S. Allen, W. Harding, and P. Mansfield, *J. Phys. C* **5**, L89 (1972).
- ²⁸D. S. Metzger and J. R. Gaines, *Phys. Rev.* **147**, 644 (1966).
- ²⁹For further details on this work see W. E. Carlos and P. C. Taylor, *J. Phys. (Paris)* **42**, C4-725 (1981).
- ³⁰J. A. Reimer, R. W. Vaughan, and J. C. Knights, *Solid State Commun.* **37**, 161 (1981).
- ³¹C. C. Tsai, H. Fritzsche, M. H. Tannelian, P. G. Gaczi, P. O. Persons, and M. A. Vesaghi, in *Amorphous and Liquid Semiconductors*, edited by W. E. Spear (University of Edinburgh, Edinburgh, 1977), p. 339.
- ³²D. E. Carlson and R. W. Griffith (private communications).
- ³³C. P. Slichter, *Principles of Magnetic Resonance* (Springer, New York, 1980), p. 137.
- ³⁴A. Abragam, *The Principles of Nuclear Magnetism*, Ref. 20, p. 378.
- ³⁵M. Rubinstein, H. A. Reising, T. L. Reinecke, and K. L. Ngai, *Phys. Rev. Lett.* **34**, 1444 (1975).
- ³⁶M. S. Conradi, K. Luszczynski, and R. E. Norberg, *Phys. Rev. B* **20**, 2594 (1979).
- ³⁷E. Crammer and M. Polanyi, *Z. Phys. Chem. (Leipzig)* **B 21**, 459 (1933); K. Matizuki and T. Nagamiya, *J. Phys. Soc. Jpn.* **11**, 93 (1956); A. J. Berhovsky and W. N. Hardy, *Phys. Rev. B* **8**, 5013 (1973).
- ³⁸P. A. Fedders, *Phys. Rev. B* **20**, 2588 (1979).
- ³⁹J. van Kranendonk, *Physica (Utrecht)* **20**, 781 (1954).
- ⁴⁰See, for example, S. Hunklinger and W. Arnold, *Physical Acoustics* (Academic, New York, 1976), Vol. 12, p. 155; J. E. Graebner and B. Golding, *Phys. Rev. B* **15**, 964 (1979).
- ⁴¹T. L. Reinecke and K. L. Ngai, *Phys. Rev. B* **12**, 3476 (1975).
- ⁴²M. Von Haumeder, U. Strom, and S. Hunklinger, *Phys. Rev. Lett.* **44**, 84 (1980).
- ⁴³B. A. Scott, R. M. Plecenik, and E. E. Simoyi, *Appl. Phys. Lett.* **39**, 73 (1981).
- ⁴⁴F. J. Kampar and R. W. Griffith, *Appl. Phys. Lett.* **39**, 407 (1981).